

“Full Fusion” is not Ineluctable during Vesicular Exocytosis of Neurotransmitters by Endocrine Cells

Alexander Oleinick, Irina Svir, Christian Amatore*

Ecole Normale Supérieure-PSL Research University, Département de Chimie, Sorbonne Universités-UPMC Univ. Paris 06, CNRS UMR 8640 PASTEUR, 24 rue Lhomond, 75005 Paris, France.

Supplementary material

Eqn (6) and its applications presented in the main text are entirely original. However, they strongly rely on a model that has been progressively elaborated in a series of previous published works that were validated through precise confrontations with experimental amperometric spikes [1-3]. However, before the existence of Eqn (6), extracting the fusion pore dynamics after its SNAREs-constrained initial stage required delicate and time-consuming auto-adaptive numerical procedures that had to be performed under constant control by the operator. This has certainly been essential in the progress of our present understanding and for validating the present analytical approach but prevented any fast and automatic treatment of large series of amperometric spikes as is required to accumulate statistically significant.

So, it is the purpose of sections SM1 and SM2 to recall the main characteristics of this model and the assumptions on which it rests. These results are not original and have been already published by elements so they could not be incorporated in the main manuscript. However, we believe that it would be helpful to readers to find them summarized in a single document. Nonetheless, readers are encouraged to examine our previous reports [1-3] in which the elements of these detailed analyses were reported and extensively validated.

Sections SM3 reports the experimental conditions and provides a summary of the main statistical features of the amperometric spikes that have been already reported and discussed [4, 5] but are used anew in this work based on Eqn (6) in order to extract the fusion pore characteristics and dynamics reported and discussed in the main text. Nonetheless, readers are encouraged to examine our previous reports [4, 5] in which the original data have been published.

SM1. Physico-mathematical description of the model leading to Eqn (6) [1-3].

We consider that an exocytotic vesicle of radius R_{ves} is connected at time $t = 0$ to the extracellular fluid by a lipidic channel (the fusion pore) of internal radius R_{pore} and length L . Catecholamine cations stored in the vesicle dense core matrix may thus be released and diffuse extremely fast (i.e., in a few tens of a microsecond) across the artificial synaptic cleft created between the cell membrane surface and that of a closely (ca. 100 nm) positioned carbon fibre electrode, where they are detected through their two-electron oxidation, hence generating an amperometric current $i(t) = -2F(dq_{\text{ves}}/dt)$ [6], where F is the Faraday and q_{ves} the quantity (moles) of releasable catecholamines still contained inside the matrix at time t .

Inside the matrix, the transport of the catecholamine cations involves a combination of physical diffusion[7-9] (i.e., in the sense of Einstein-Schmoluchowski) through tortuous paths[10] and site-hopping[11-21] between occupied and freed sites of the polyanionic chromogranins strands as occurs in polymers and gels [15-20]. This second contribution is governed by microscopic and macroscopic laws that are identical to those of physical diffusion with an equivalent diffusion coefficient whose value is given by $\langle \mu^2 \rangle \cdot \langle \nu \rangle$ where $\langle \mu^2 \rangle$ is the mean squared distance between two sites and $\langle \nu \rangle$ the mean frequency of exchange between sites [11-21]. These two contributions add. Hence, one may consider that transport occurs by diffusion in an extended sense with an equivalent diffusion coefficient D_{ves} that integrates all those contributions.

In a general case, the released flux is kinetically regulated by:

- The intrinsic rate constant $\kappa = D_{\text{ves}}/R_{\text{ves}}^2$ within the matrix,
- The radius of the fusion pore, R_{pore} , that impose a convergent diffusion within the matrix towards the fusion pore entrance,
- The rate of transport across the length, L , of the fusion pore channel.

Let us first consider the last item. Inside the channel, that is assumed to be filled with the extracellular fluid, catecholamines cations are transported by a combination of physical diffusion (i.e., in the sense of Einstein- Schmoluchowski)[7-9] and of electroosmotic flow. Indeed, while the fusion pore retains a nanometric radius, the pH gradient (ca. 5 inside the matrix, vs. ca. 7.2 in the extracellular fluid)[22] induces an electroosmotic driving force[23] operating in the same direction as diffusion, i.e., towards the extracellular fluid.

The intrinsic rate physical diffusion in the channel is $\kappa_{\text{ch}} = D_{\text{ch}}/L^2$ where D_{ch} can be taken as close to the diffusion coefficient in aqueous media (i.e., $D_{\text{ch}} \approx 5 \times 10^{-6} \text{cm}^2 \text{s}^{-1}$) as soon as the channel is wider than ca. 2 nm [24-26]. Hence, $\kappa_{\text{ch}} \approx 10^8 (5/l^2) \text{s}^{-1}$ where l is the value of L in nanometers. This shows that in order κ_{ch} to be kinetically limiting vs. the rate of diffusion inside the matrix, i.e., that $\kappa_{\text{ch}} \leq \kappa$, in chromaffin cells for which $\kappa = D_{\text{ves}}/R_{\text{ves}}^2 = 415 \text{s}^{-1}$ has been determined [3], the fusion pore channel should have a length of at least ca 10^3 nm. Even if D_{ch} resulted only one tenth of its value in the bulk, the channel length would still have to be ca.

100 nm to be limiting. Both figures seem clearly unrealistic.

Furthermore, this diffusional contribution is superimposed onto the electroosmotic drive, so that the rate of expulsion of catecholamine cations through the fusion pore channel results even larger than κ_{ch} .

Hence, one may safely consider that the transport of catecholamines along the fusion pore channel is not limiting. It ensues that the released flux is only limited by the convergent diffusion of catecholamine cations towards the fusion pore entrance inside the matrix [3].

SM2. Achievement of a quasi-steady state concentration regime within the matrix[1-3].

The diffusion wave created by the fusion pore opening expands inside the matrix with a rate $\kappa = D_{ves}/R_{ves}^2 = 415 \text{ s}^{-1}$ [3]. This diffusion wave spans over the complete interior of the matrix in a few tenths of a millisecond after the fusion pore opening, as is evidenced in Figure SM-1 that represents the concentration profiles achieved at different times $\theta = \kappa t$ along one diameter of a spherical matrix, i.e., along the longest diffusional pathway within the matrix.

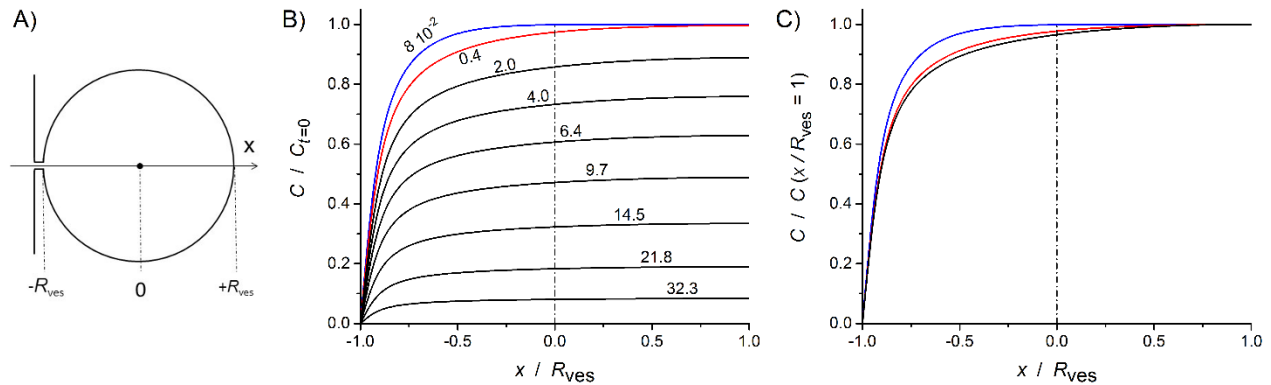


Figure SM-1.(A) Schematic representation of the geometry of a fused vesicle with definition of the diametric axis x . (B) Concentration profiles established at different $\kappa t = D_{ves} t/R_{ves}^2$ values (as indicated on each curve) assuming that the fusion pore opened instantly at its maximal radius of $0.87R_{ves}$ (i.e., at a 5 degree half-cone angle). (C) Same concentration profiles as in (B) but normalized to the concentration value at $x/R_{ves} = 1$, shown using the same colour code as in (B); note that all curve shown in black colour in (B) strictly superimpose in (C).

Figure SM-1 shows that as soon as the diffusion wave hits the vesicle membrane placed diametrically opposite to the pore, the concentration profiles at different times are homothetic (compare to panel C) [1, 27-29]. In other words the diffusion pattern reaches a quasi-steady state regime as soon as $\kappa t > 0.1$ even for the most severe condition considered here, viz., involving a rather large instant opening of the fusion pore (5 degrees, viz., at a ca. 13.6 nm radius for a vesicle of mean radius $R_{ves} = 156 \text{ nm}$). Note that for $\kappa t = 0.4$ (red curve), the mean deviation from the quasi-steady state regime is ca. 1%, i.e., much less than the precision on the

amperometric current measurements. Hence, when the fusion pore opens gradually to its maximal radius (as observed in Figure 1A in main text) $\kappa t > 0.1$ is sufficient to ensure that the quasi-steady state regime is achieved.

As soon as this quasi-steady state is established, at any time the concentration at any point becomes proportional to its average value within the matrix, the local scaling factor depending only on the location in the matrix but being independent of time (compare Figure SM-1C). It then follows that at any time, t , the flux of catecholamine cations through the fusion pore (i.e., the concentration gradient at the entrance of the pore) is proportional to the average quantity, $q_{\text{ves}}(t)$, of releasable catecholamines still present at the same time t .

Finally, when the quasi steady-state convergent diffusion regime is achieved, and the pore radius small as compared to that of the vesicle, the laws of diffusion establish that the flux exiting through the pore is proportional to the pore radius perimeter, $2\pi R_{\text{pore}}$, rather than its surface area, the diffusion coefficient, D_{ves} , and to the difference of concentrations values between the matrix and the pore entrance [30]. Since transport through the channel length and across the artificial electrode-cell cleft are extremely fast vs. that within the matrix, the concentration at the pore entrance is negligible vs that in the matrix up to the very end of release. Finally, since the volume of the matrix may be considered constant owing to its constriction by its membrane, the concentration inside the matrix is proportional to $q_{\text{ves}}(t)$, which validates Eqn (1) in the main text.

SM3. Experimental conditions and characteristics of amperometric spikes observed under controls, hyper- and hypotonic, AA- and LPC-modified conditions [4, 5].

The amperometric spikes used in this work and analysed using Eqn (6) were recorded at carbon fibre microelectrodes from chromaffin cells under normal conditions or after their membranes were briefly submitted to different perturbations with the purpose of changing their tensions and viscosities. These data have already been the subject of two previous reports [4, 5], though at the time of their publication they could only be characterized and discussed in a classical mode, i.e., based on the values of their maximum current intensity (I_{max}), charge (Q) and half-life times ($t_{1/2}$). These published data are summarized in Table SM-1 to facilitate the reader's task. Note that under each condition the numbers of spikes analysed in the present study (Figures 2 and 3 of the main text) are smaller than in the previous reports because only the spikes displaying perfect single-exponential decay branches were retained and treated through Eqn (6), while those analysed in references [4, 5] encompassed spikes with single-, double- and mixed exponential modes of decay.

Main experimental conditions [4, 5]

Vesicular release was elicited from bovine chromaffin cells by 2mM Ba^{2+} (in Locke buffer supplemented with 0.7 mM MgCl_2 , without carbonates) injection during 2s. Amperometric spikes were recorded at 7 μm diameter carbon fiber microelectrodes held at 0.65 V vs. Ag/AgCl.

Controls spikes (311 spikes from 5 cells) were measured under isotonic conditions (315 mOsm: 154 mM NaCl, 4.2 mM KCl, 0.7 mM MgCl₂, 11.2 mM glucose, 10 mM HEPES, pH 7.4). For measurements under hypertonic conditions the cells were submitted to a brief pulse of the same solution in which NaCl concentration was adjusted at a 750 mOsm osmotic pressure (42 spikes from 6 cells). For measurements under hypotonic conditions the cells were submitted to a brief pulse of the same solution in which NaCl concentration was adjusted at a 200 mOsm osmotic pressure (100 spikes from 5 cells).

To investigate the effect of AA or LPC, the cells were incubated during 3 min before monitoring release with 20 μM AA in isotonic buffer (145 spikes from 5 cells) or 2 μM LPC in isotonic buffer (229 spikes from 6 cells).

Table SM-1. Summary of the main characteristics of the amperometric spikes already reported in references [4, 5]. Carbon fibre electrodes (7 μm diameter); see original publications for more detailed experimental conditions. Not all these spikes were analysed in the present work since only spikes exhibiting perfect single-exponential decay branches were retained.

Conditions	I_{\max} / pA	Q / fC	$t_{1/2}$ / ms
Controls-2 (532 spikes, 5 cells)	24.3±1.8	975±65	40.2±1.5
Hypertonic (750 mOsm; 380 spikes, 6 cells) ^[4]	n.d.	395±40	n.d.
Hypotonic (200 mOsm; 457 spikes, 5 cells) ^[4]	30.8±1.7	1420±80	43.0±1.1
AA-modified (380 spikes, 6 cells) ^[5]	10±1	590±50	53.5±1.5
LPC-modified (590 spikes, 5 cells) ^[5]	43.7±2.1	1600±70	32.1±0.6

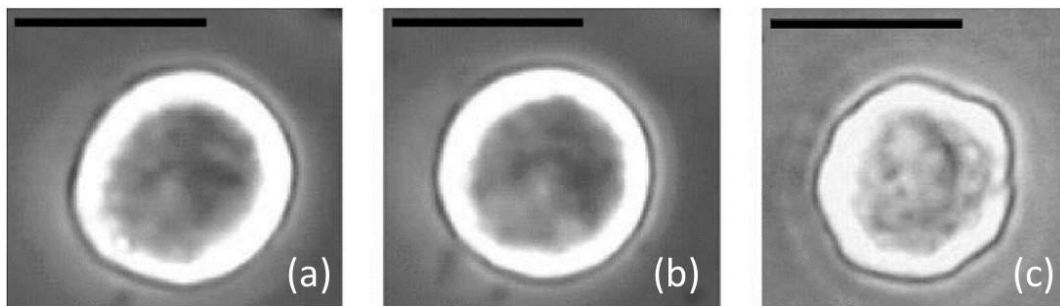


Figure SM-2. Micrographs of chromaffin cells under isotonic (control) conditions (a) or immediately after being submitted to a brief hypotonic (b) or hypertonic (c) shock (see Table SM-1). The bar in each panel represents 10 μm. Adapted from Reference [4].

References for Supporting Material

- [1] Amatore C, Oleinick AI, Svir I. 2010 Diffusion from within a spherical body with partially blocked surface: diffusion through a constant surface area. *ChemPhysChem***11**, 149-158. (doi: 10.1002/cphc.200900646)
- [2] Amatore C, Oleinick AI, Svir I. 2010 Reconstruction of aperture functions during full fusion in vesicular exocytosis of neurotransmitters. *ChemPhysChem***11**, 159-174. (doi: 10.1002/cphc.200900647)
- [3] Oleinick A, Lemaître F, Guille-Collignon M, Svir I, Amatore C. 2013 Vesicular release of neurotransmitters: converting amperometric measurements into size, dynamics and energetics of initial fusion pores. *Faraday Discuss.***164**, 33-55. (doi: 10.1039/c3fd00028a)
- [4] Amatore C, Arbault S, Bonifas I, Lemaître F, Verchier Y. 2007 Vesicular exocytosis under hypotonic conditions shows two distinct populations of dense core vesicles in bovine chromaffin cells. *ChemPhysChem***8**, 578-585. (doi: 10.1002/cphc.200600607)
- [5] Amatore C, Arbault S, Bouret Y, Guille M, Lemaître F, Verchier Y. 2006 Regulation of exocytosis in chromaffin cells by trans-insertion of lysophosphatidylcholine and arachidonic acid into the outer leaflet of the cell membrane. *ChemBioChem***7**, 1998-2003. (doi: 10.1002/cbic.200600194)
- [6] The factor 2 in stems from the fact that the electrooxidation of catecholamine cations at the carbon fiber microelectrode surface involves a $2e^-/2H^+$ process. See: Ciolkowski EL, Maness KM, Cahill PS, Wightman RM, Evans DH, Fosset B, Amatore C. 1994 Disproportionation during electrooxidation of catecholamines at carbon-fiber microelectrodes. *Anal. Chem.* **66**, 3611-3617. (doi: 10.1021/ac00093a013)
- [7] Crank J. 1975 *The Mathematics of Diffusion*. Clarendon Press, Oxford. 2nd Edn, ppf. 89.
- [8] Tikhonov AN, Samarskii AA. 1966 *Equations of Mathematical Physics*. Science, Moscow.
- [9] Polyanin AD, Vyazmin AV, Zhurov AI, Kazenin DA. 1998 *Handbook of Exact Solutions of Heat and Mass Transfer Equations*. Factorial, Moscow.
- [10] See e.g.: Wightman RM, Amatore C, Engstrom RC, Hale PD, Kristensen EW, Kuhr WG, May LJ. 1988 Real-time characterization of dopamine overflow and uptake in the rat striatum. *Neuroscience***25**, 513-523. (doi: 10.1016/0306-4522(88)90255-2)
- [11] Transport inside a still compact matrix may not proceed through classical diffusion (i.e., in the Einstein-Schmoluchowski sense) but through hopping between occupied and free sites. However, such "site-hopping" processes give rise to the same microscopic and macroscopic laws as classical diffusion. See, e.g., references [12-21].
- [12] Dahms HJ. 1968 Electronic conduction in aqueous solution. *J. Phys. Chem.***72**, 362-364. (doi: 10.1021/j100847a073)
- [13] Ruff I, Friedrich VJ. 1971 Transfer diffusion. I. Theoretical. *J. Phys. Chem.***75**, 3297-3302. (doi: 10.1021/j100690a016)

- [14] Ruff I, Friedrich VJ, Demeter K, Csillag K. 1971 Transfer diffusion. II. Kinetics of electron exchange reaction between ferrocene and ferricinium ion in alcohols. *J. Phys. Chem.***75**, 3303-3309. (doi: 10.1021/j100690a017)
- [15] Murray RW, Goodenough JB, Albery WJ. 1981 Modified electrodes: chemically modified electrodes for electrocatalysis [and discussion]. *Phil. Trans. R. Soc., London A.*, **302**, 253-265. (doi: 10.1098/rsta.1981.0165)
- [16] Andrieux CP, Savéant JM. 1980 Electron transfer through redox polymer films. *J. Electroanal. Chem.***111**, 377-381. (doi: 10.1016/S0022-0728(80)80058-1)
- [17] Laviron E. 1980 A multilayer model for the study of space distributed redox modified electrodes: Part I. Description and discussion of the model. *J. Electroanal. Chem.***112**, 1-9. (doi: 10.1016/S0022-0728(80)80002-7)
- [18] Blauch DN, Savéant JM. 1992 Dynamics of electron hopping in assemblies of redox centers. Percolation and diffusion. *J. Am. Chem. Soc.***114**, 3323-3332. (doi: 10.1021/ja00035a025)
- [19] Blauch DN, Savéant JM. 1993 Effects of long-range electron transfer on charge transport in static assemblies of redox centers. *J. Phys. Chem.***97**, 6444-6448. (doi: 10.1021/j100126a019)
- [20] Amatore C, Bouret Y, Maisonhaute E, Goldsmith JI, Abruña HD. 2001 Ultrafast voltammetry of adsorbed redox active dendrimers with nanometric resolution: an electrochemical microtome. *ChemPhysChem***2**, 130-134. (doi: 10.1002/1439-7641(20010216)2:2<130::AID-CPHC130>3.0.CO;2-K)
- [21] Amatore C, Bouret Y, Maisonhaute E, Goldsmith JI, Abruña HD. 2001 Precise adjustment of nanometric-scale diffusion layers within a redox dendrimer molecule by ultrafast cyclic voltammetry: an electrochemical nanometric microtome. *Chem. Eur. J.* **7**, 2206-2226. (doi: 10.1002/1521-3765(20010518)7:10<2206::AID-CHEM2206>3.0.CO;2-Y)
- [22] See e.g.: Borges R, Pereda D, Beltran B, Prunell M, Rodriguez M, Machado JD. 2010 Intravesicular factors controlling exocytosis in chromaffin cells. *Cell. Mol. Neurobiol.***30**, 1539-1364. (doi: 10.1007/s10571-010-9589-6)
- [23] For a recent investigation of the effect of pH gradient on increasing or decreasing the transport rate of ions in nanopores see e.g.: Yang M, Yang XH, Wang KM, Wang Q, Fan X, Liu W, Liu XZ, Liu JB, Huang J. 2015 Tuning transport selectivity of ionic species by phosphoric acid gradient in positively charged nanochannel membranes. *Anal. Chem.***87**, 1544-1551. (doi: 10.1021/ac503813r)
- [24] In aqueous electrolytes containing salt at concentrations similar to physiological medium, the thickness of double layers near a charged wall is less than 1 nm based on Gouy-Chapman-Stern theory. For pores that have radii less than this value, this is expected to induce specific effects that modify the transport across the fusion pore channel. See e.g. [25]. However, for larger pores such effects are not sufficient to alter significantly the diffusion coefficient vs. that in the bulk solution. See e.g. [26].

- [25] Hocine S, Hartkamp R, Siboulet B, Duvail M, Coasne B, Turq P, Dufreche JF. 2016 How ion condensation occurs at a charged surface: a molecular dynamics investigation of the stern layer for water–silica interfaces. *J. Phys. Chem. C* **120**, 963-973. (doi: 10.1021/acs.jpcc.5b08836)
- [26] Bourg IC, Steefel CI. 2012 Molecular dynamics simulations of water structure and diffusion in silica nanopores. *J. Phys. Chem. C* **116**, 11556-11564. (doi: 10.1021/jp301299a)
- [27] The same occurs for a swelling-wave propagation inside a spherical particle; see [28]. However, would swelling be the cause of release rather than diffusion, the time dependence of the flux would result different; see [29].
- [28] Tanaka T, Fillmore DJ. 1979 Kinetics of swelling of gels. *J. Chem. Phys.* **70**, 1214-1218. (doi: 10.1063/1.437602)
- [29] Oleinick A, Hu R, Ren B, Tian ZQ, Svir I, Amatore C. 2016 Theoretical model of neurotransmitter release during in vivo vesicular exocytosis based on a grainy biphasic nano-structuration of chromogranins within dense core matrixes. *J. Electrochem. Soc.* **163**, H3014-H3024. (doi: 10.1149/2.0031604jes)
- [30] See e.g.: Amatore C, Fosset B. 1996 Equivalence between microelectrodes of different shapes: between myth and reality. *Anal. Chem.* **68**, 4377-4388. (doi: 10.1021/ac960421s)